IAA Technology Development Center Report

Dmitry Marshalov, Evgeny Khvostov, Maxim Zotov, Dmitrii Ivanov, Vladimir Bykov, Victor Stempkovskiy, Alexander Shishikin, Vitaliy Chernov, Sergey Grenkov, Anton Berdnikov, Leonid Fedotov, Alexey Melnikov, Ilia Pozdnyakov, Ismail Rahimov, Igor Shakhnabiev, Alexey Lavrov, Yury Vekshin

Abstract The main activities of the IAA Center for Technological Development in 2023–2024 were focused on the work with a mobile VLBI station prototype and modernization of the Multifunctional Digital Backend system for upgrading 32-m radio telescope equipment. This report provides a brief overview of these activities.

1 Transportable VLBI Station

In 2024, IAA RAS was responsible for the development and construction of a compact VLBI station, which was designed to be easily transported and deployed at various locations. The transportable VLBI station is equipped with a 4.3-m antenna (see Figure 1) that is fully steerable, in addition to all the necessary equipment for VLBI technology.

The RT-4 antenna is constructed using a Cassegrain design and is equipped with a 0.8-meter sub-reflector. The RT-4 antenna system has a capacity for movement within azimuths from -90° to $+450^\circ$ and elevations 5° to 85°. The maximum azimuth slew rate is 2°/s, while the elevation slew rate is 0.5°/s. A functional diagram of the transportable VLBI station is presented in Figure 2.

The transportable VLBI radio telescope has been equipped with a dual-band S/X receiver (see Figure 3). The receiver has been engineered to provide signal reception within the 2.2–2.6 GHz and 8.1–9.2 GHz bands, and it is able to amplify and convert the signal to the IF band. The noise temperature of the receiver is less than 20 K in both frequency bands.

Fig. 1 Transportable VLBI station.

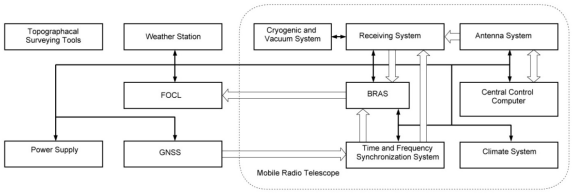

Fig. 2 Functional diagram of transportable VLBI station.

The dual-band S/X feed (Figure 4) was developed and manufactured, thereby ensuring optimal field formation at the reflector aperture. In the S-band, the feed is a corrugated horn antenna excited by four coaxial-to-waveguide transitions. The X-band dielectric feed is excited via a circular waveguide. The dielectric feed was designed to form the required beam width. The VSWR of the feed has been measured and found to be

Institute of Applied Astronomy (IAA RAS)

IAA Technology Development Center

IVS 2023+2024 Biennial Report

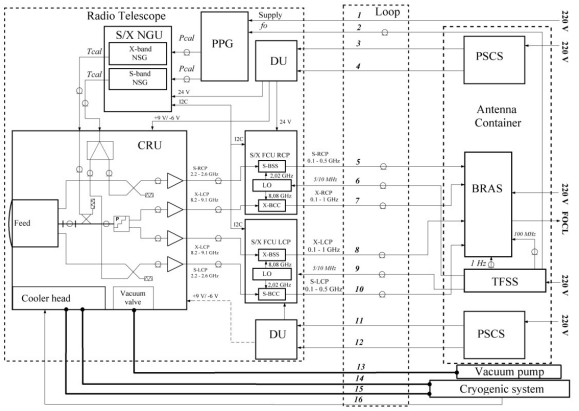

Fig. 3 . Functional diagram of the Receiving System: Cryogenic Receiver Unit (CRU), Noise Generator Unit (NGU), Frequency Converter Unit (FCU), Broadband Acquisition System (BRAS), Time-and-Frequency Synchronization System (TFSS), Noise Signal Generator (NSG), Picosecond Pulse Generator (PPG), Power Supply and Control System (PSCS), and Distribution Unit (DU).

no greater than 1.42 in the S-band and 1.18 in the X-band. The optimized design keeps cross-polarization at 11% and spillover at 6%.

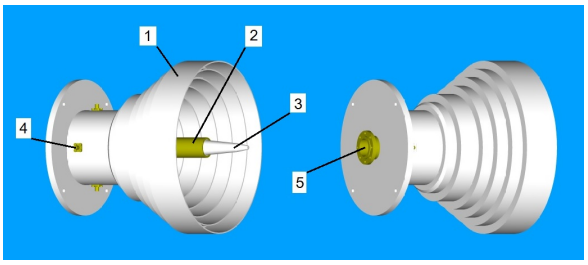

Fig. 4 Dual-band feed.

It was necessary to devise a solution to the problem of the feed extending beyond the dewar. The solution was to design a special multilayer vacuum window. The geometry of the window structure (see Figure 5) was calculated to minimize reflective losses in X-band.

In the S-band, the unit responsible for the formation of circular polarization is comprised of a quadrature hybrid and two directional couplers that are 180 degrees apart. The integration of all couplers into a single printed circuit board (PSB) (see Figure 6) resulted in a reduction of system noise temperature, a minimization of amplitude-phase imbalance, and an enhancement of

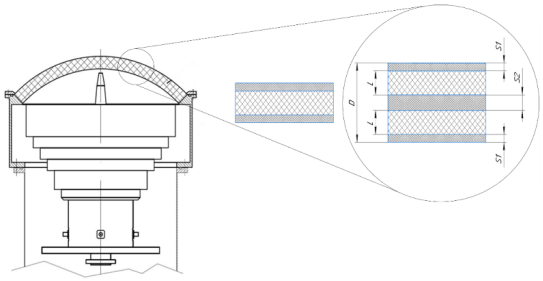

Fig. 5 Aperture assembly and vacuum window structure.

the feed's axial ratio. The operating bandwidth circular polarization forming unit is approximately 54%, with amplitude and phase imbalance not exceeding ± 0.75 dB and ± 3–4 degrees, respectively. The implementation of the aforementioned scheme resulted in a reduction of the noise temperature from 16 K to 13–14 K in comparison to a scheme using discrete couplers.

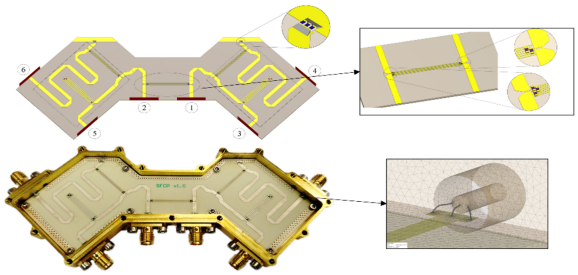

Fig. 6 PCB of circular polarization forming unit (top) and the one installed inside the cryogenic block (bottom).

In order to achieve a temperature of 15 Kelvin in the feed and low noise amplifiers (LNAs) of the CRU, a cryogenic vacuum system is employed. The generation of calibration signals is facilitated by the NGU and PPG, which are subsequently injected by directional couplers situated prior to the primary signal handling unit. The signals from the CRU outputs are then directed to dual-band FCUs, with each FCU operating on a distinct polarization band. In this instance, the high-frequency signal is amplified and converted to the intermediate frequency (IF) band. The signals from the FCU outputs are transmitted via radio frequency cables to the corresponding inputs of the recording system. BRAS is utilized as the backend for Transportable VLBI.

In order to function correctly, it is imperative that the receiving and recording equipment be supplied with reference time and frequency signals. These include GNSS time scale signals and local station time scale signals, as well as reference harmonic signals of 5 MHz, 10 MHz, and 100 MHz. The frequency and time synchronization system (TFSS) responsible for this function is illustrated in Figure 7.

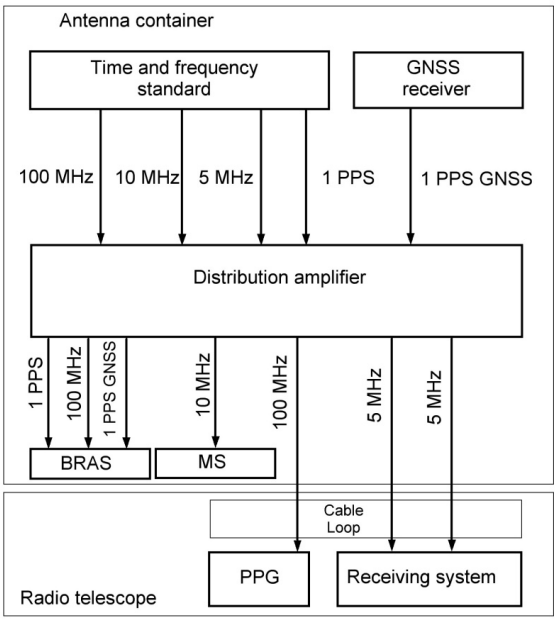

Fig. 7 Functional diagram of TFSS.

During the trial operation, the transportable VLBI station was connected to the Svetloe Observatory LAN. This facilitated the transfer of observational data from transportable VLBI to the Collective Use Center (CUC) of the RAS. Radiometric observations of Cassiopeia A and Cygnus A sources were conducted. The system noise temperature, SEFD, and efficiency of the RT-4 radio telescope of transportable VLBI were determined (see Table 1).

The transportable station participated in joint VLBI observations as part of the "Quasar" VLBI Network. After the observations, the station coordinates were refined to an accuracy of 10 mm. In the future, the implementation of a transportable VLBI station has the potential to facilitate the expansion of the "Quasar" VLBI Network into regions that are currently inaccessible, thereby enhancing the precision of VLBI observations.

Table 1 Transportable VLBI station characteristics.

	T_{REC}, K		T_{SYS}, K		SEFD, Jy		A_{eff}	
	Calc.	Meas.	Calc.	Meas.	Calc.	Meas.	Calc.	Meas.
S_{RCP}	25	16	47	47	18000	18300	0.52	0.50
S_{LCP}	25	16	47	48	18000	18300	0.52	0.50
X_{RCP}	25	17	37	42	14000	15300	0.55	0.54
X_{LCP}	25	18	37	40	14000	13700	0.55	0.57

2 Multifunctional Digital Backend System

In accordance with the development plans outlined in the previous report [1], the equipping of the "Quasar" VLBI Network radio telescopes with Multifunctional Digital Backend (MDBE) systems was successfully completed on schedule.

In 2023, 8-channel MDBEs were installed and commissioned for regular operation on the RT-13 radio telescopes at the Zelenchukskaya and Badary observatories, fully replacing the previously used wideband signal processing units [2]. Modified 4-channel MDBEs [3], including intermediate-frequency (IF) distribution modules, were installed on the RT-32 radio telescopes (see Figure 8) at all three observatories (Svetloe, Zelenchukskaya, and Badary). By the end of 2023, the entire "Quasar" VLBI Network was thus equipped with modern, universal digital signal processing systems.

Fig. 8 MDBE for the RT-32 radio telescope.

A key achievement of the reporting period was the development, testing, and implementation of new firmware for the MDBE's field-programmable gate arrays (FPGAs), which significantly expanded system functionality. The updated firmware currently supports four principal operational modes:

- **Wideband VLBI modes** [4]: operating at 2048, 1024, and 512 MHz, producing VDIF-format data streams with one- or two-bit quantization (up to 4096, 2048, or 1024 Mbps per channel, depending on configuration);
- **Narrowband VLBI modes** [6]: enabling the registration of up to 16 independently tunable channels with bandwidths of 0.5–32 MHz. Both one- and two-bit quantization are supported (up to 2048 Mbps in VDIF format). This mode provides full compatibility with international VLBI networks and has initiated the phased decommissioning of the obsolete P1002M systems. Additional one-channel firmware (64 and 128 MHz) was developed for radar observation programs;
- **Spectrally selective radiometer modes** [6]: designed for radiometric observations and calibration under strong radio frequency interference (RFI), particularly in the L- and S-bands. This mode allows real-time identification and exclusion of interference-contaminated spectral regions, thereby improving measurement reliability. Supported recording bandwidths are 2048, 1024, and 512 MHz;
- **Spectrometer mode firmware** [7]: providing high-resolution spectral line registration (e.g., OH and H_2O masers) with frequency resolution down to 61 Hz. Advanced algorithms for interference suppression enable successful observations even in heavily congested frequency bands.

The effectiveness of the upgraded MDBE was validated through numerous test and scheduled observing sessions. In particular, comparative geodetic VLBI experiments with the MDBE and the legacy P1002M system on the RT-32 telescope at Svetloe demonstrated that MDBE-based results were fully consistent and, in certain parameters (such as the stability of Universal Time correction estimates), even superior.

The MDBE control software has been integrated into the standard telescope central computer system (based on the Field System software packge), ensuring operational simplicity and seamless participation in international VLBI campaigns.

By 2025, the MDBE had become the universal platform for all observation types within the "Quasar" VLBI Network, replacing a diverse array of specialized systems (P1002M, spectrometers, radiometers). This unification not only streamlined hardware management but also opened new research opportunities thanks to the system's high flexibility and wide recording bandwidth. Future development will focus on continued software support and the implementation of additional modes, including spacecraft signal reception and pulsar observations.

References

1. D. Marshalov, E. Nosov, G. Ilin, E. Khvostov, V. Bykov, A. Isaenko, V. Stempkovskiy, A. Shishikin, IAA Technology Development Center Report for 2019 – 2020, in: International VLBI Service for Geodesy and Astrometry 2019+2020 Biennial Report, edited by D. Behrend, K. L. Armstrong, and K. D. Baver, NASA/TP-20210021389, pp. 279–282, 2021.
2. D. Marshalov, S. Grenkov, N. Koltsov et al., Universal digital signal processing system for radio telescopes, in: Transactions of IAA RAS. Vol. 71, pp. 9 – 17, 2024. https://doi.org/10.32876/ApplAstron.71.9–17
3. D. Marshalov, A. Berdnikov, S. Grenkov, L. Fedotov, Yu. Sheinman, A. Mikhailov, A. Ustinov, I. Rahimov, A. Isaenko, Modernization of the RT-32 radio telescope data acquisition system in Svetloe observatory, in: Transactions of IAA RAS. Vol. 70, pp. 39–49, 2024. https://doi.org/10.32876/ApplAstron.70.39–49
4. D. Marshalov, E. Nosov, L. Fedotov, Y. Sheynman, Multifunctional digital backend for RT-13 radio telescope at Svetloe observatory, in: Transactions of IAA RAS. Vol. 56, pp. 39–47, 2021. https://doi.org/10.32876/ApplAstron.56.39–47
5. S. Grenkov, A. Melnikov, L. Fedotov, Narrow-band operation mode of the Multifunctional Digital Backend system, in: Transactions of IAA RAS. Vol. 72, pp. 20–32, 2025. https://doi.org/10.32876/ApplAstron.72.20–32
6. S. Grenkov, L. Fedotov, Spectral-selective radiometric recording by means of Multifunctional Digital Backend system, in: Transactions of IAA RAS. Vol. 62, pp. 3–9, 2022. https://doi.org/10.32876/ApplAstron.62.3–9
7. S. Grenkov, I. Rahimov, L. Fedotov, Registration of narrowband cosmic radio emissions with Multifunctional Digital Backend system, in: Transactions of IAA RAS. Vol. 66, pp. 11–17, 2023. https://doi.org/10.32876/ApplAstron.66.11–17
8. E. Nosov, E. Khvostov, A. Vytnov, IAA Technology Development Center Report for 2017 – 2018, in: International VLBI Service for Geodesy and Astrometry 2017+2018 Biennial Report. Edited by K. L. Armstrong, K. D. Baver, and D. Behrend, NASA/TP-2020-219041, pp. 271–274, 2020.
9. E. Nosov, D. Marshalov, L. Fedotov, Y. Sheynman, Multifunctional Digital Backend for Quasar VLBI network. *Journal of Instrumentation*, V.16, doi:10.1088/1748-0221/16/05/p05003, P05003, 2021.